# Selective Recovery of Precious Metals through Photocatalysis

**Yao Chen**
Shanghai Normal University

**Mengjiao Xu**
Shanghai Normal University

**Jieya Wen**
Shanghai Normal University

**Yu Wan**
Shanghai Normal University

**Qingfei Zhao**
Shanghai Normal University

**Xia Cao**
Beijing Institute of Nanoenergy and Nanosystems

**Yong Ding**
Georgia Institute of Technology

**Zhong Wang**
Georgia Institute of Technology

**Hexing Li** ( ✉ hexing-li@shnu.edu.cn )
Shanghai Normal University

**Zhenfeng Bian**
Shanghai Normal University    https://orcid.org/0000-0001-7552-8027

---

**Article**

# Selective Recovery of Precious Metals through Photocatalysis

Yao Chen[1], Mengjiao Xu[1], Jieya Wen[1], Yu Wan[1], Qingfei Zhao[1], Xia Cao[3], Yong Ding[4], Zhong Lin Wang[3,4*], Hexing Li[1,2*] & Zhenfeng Bian[1*]

[1] MOE Key Laboratory of Resource Chemistry and Shanghai Key Laboratory of Rare Earth Functional Materials, Shanghai Normal University, Shanghai 200234, China.

[2] Shanghai University of Electric Power, Shanghai 200090, China.

[3] Beijing Institute of Nanoenergy and Nanosystems, Chinese Academy of Sciences, Beijing 100083, China.

[4] School of Materials Science and Engineering, Georgia Institute of Technology, Atlanta, Georgia 30332-0245, United States.

**Precious metals such as gold and platinum are valued materials for a variety of important applications, but their scarcity poses a risk of supply interruption. However, the dissolution and recovery of precious metals using the current methods are limited by associated serious environmental pollution and high energy consumption. Here, we show a photocatalytic process that allows one to selective retrieve 7 kinds of precious metal elements (Ag, Au, Pd, Pt, Ru, Rh and Ir) (with dissolution efficiency of 99%) from waste circuit boards, ternary automotive catalysts and even ores. Precious metals is recovered with high purity (≥98%) through a simple reductive method. The whole process only needs light and catalyst without strong acid, strong base and highly toxic cyanide. It has an environmentally friendly, scalable and efficient way, in which the catalyst has been recycled more than 100 times under normal temperature and pressure without performance degradation. It has successfully realized the scale of dissolution from grams to kilograms, and it is expected to realize large-scale recovery of precious metals in industrial application. This general approach provides an unprecedent technology for recycling resources on earth.**

## Introduction

Precious metals (PMs) possess not only good physical properties (ductility, electrical conductivity), but also high chemical stability and strong corrosion resistance[1]. In recent years, precious metals have been increasingly used in the fields of electronic devices and modern industrial catalysis[2,3] etc. It is reported that the global demand for gold, silver and palladium in the electronics industry was about 250 tons, 12,800 tons and 40 tons, respectively[4-6]. In addition, due to the continuous development of the automobile industry, the consumption of platinum group metals is increasing[5]. The global electronic waste (e-waste) production shows that the gold content in 40 mobile phones is equivalent to one ton of ore[7]. In 2019, a total of 53.6 million tons of precious metal-containing e-waste were generated globally, including discarded computers, mobile phones and households electronic equipment[8,9]. It is a very meaningful to recycle precious metals from e-waste and waste catalyst.

It remains a grand challenge to mine and retrieve precious metals from ores, catalysts and electronic wastes for reusage[10-13]. The recovery process of precious metal is divided into two steps: firstly, dissolve $PM^0$ into $PM^{x+}$ from electronic wastes; then reduce $PM^{x+}$ to $PM^0$ from the leachate. In the process of dissolving $PM^0$ to $PM^{x+}$, dissolution methods in the industry involving the use of corrosive and toxic aqua regia and cyanidation endanger the environment and characterized of high chemical consumption[14-18]. In view of the toxicity of aqua regia and cyanide, scientists have developed non-toxic leaching agents such as thiourea, thiosulfate and iodine to treat the dissolution of gold, but they are ineffective for the dissolution of platinum group precious metals and the operation steps are complicated (Extended Data Table 1)[18-23]. Moreover, Yang et al. used n-bromosuccinimide (NBS) and pyridine (Py) directly leached $Au^0$ waste to form $Au^{III}$ from gold ore and electronic[24]. Hong et al. used sulfuryl chloride ($SOCl_2$) and some organic solvents/reagents (pyridine, N, N-dimethylformamide and imidazole) to form "organic aqua regia" to dissolve gold and palladium[25]. The limitation of the above method is that it can only dissolve one or two precious metals and the reagent composition is complicated, which not only increases

56  the difficulty of actual operation, but also increases the cost of recovery. In the process

57  of reducing $PM^{x+}$ to $PM^0$, scientists usually design materials that can withstand acid to

58  extract precious metal ions. Hong et al. reported a porous porphyrin polymer which can

59  quantitatively capture precious metals ion from the acidic exudate of e-waste[26]. The

60  existing methods in the literature can achieve selective reduction of a precious metal.

61  Smith et al. used 1,3:2,4-dibenzylidenesorbitol as a raw material to prepare a hydrogel

62  material capable of extracting gold/silver ions[27]. Queen et al. prepared Fe-BTC/PpPDA

63  composite material, which was proven to quickly extract trace amounts of gold ion from

64  water mixtures[28]. In fact, the dissolution process of precious metals is more difficult to

65  achieve than reduction because precious metals are chemically inert, which require

66  strong oxidizing reagents.

67      It has been reported that the photocatalysis can generate highly reactive free

68  radicals in the reaction system under mild conditions. Moreover, the photocatalytic

69  technology has the advantages of simple operation, low energy consumption, no

70  secondary pollution and high efficiency. Photocatalytic oxidation has become a

71  technology of choice to tackle environmental pollution and energy crisis due to its direct

72  utilization of solar light-driven reaction and good catalyst stability. The oxidizing

73  ability of photo-generated holes ($TiO_2$ (2.91 $V_{NHE}$)) is sufficient to oxidize $PM^0$ into

74  $PM^{x+}$ (Rh (0.75 $V_{RHE}$) < Ir (0.9 $V_{RHE}$) < Pt (1.1 $V_{RHE}$) < Au (1.3 $V_{RHE}$)) [29,30]. But so far,

75  there is no report on the oxidation and dissolution of precious metals by photocatalytic

76  method.

77      Here, we have realized the use of photocatalysis to dissolve precious metals,

78  without strong acids, strong bases and toxic solvents. It has good leaching effect for 7

79  kinds of precious metals (Ag, Au, Pd, Pt, Ru, Rh and Ir). Interestingly, selective

80  dissolution of precious metals can also be achieved, providing an easy way of

81  separating these metals. More importantly, this photocatalytic technology for

82  dissolving precious metals can not only realize the recovery of noble metal nano-

83  catalysts in the laboratory, but also effectively leached precious metals from e-waste,

84  ore and automobile three-way catalyst on a large scale. To our best knowledge, this is

85　the first time that an environmental friendly photocatalysis has been applied to the

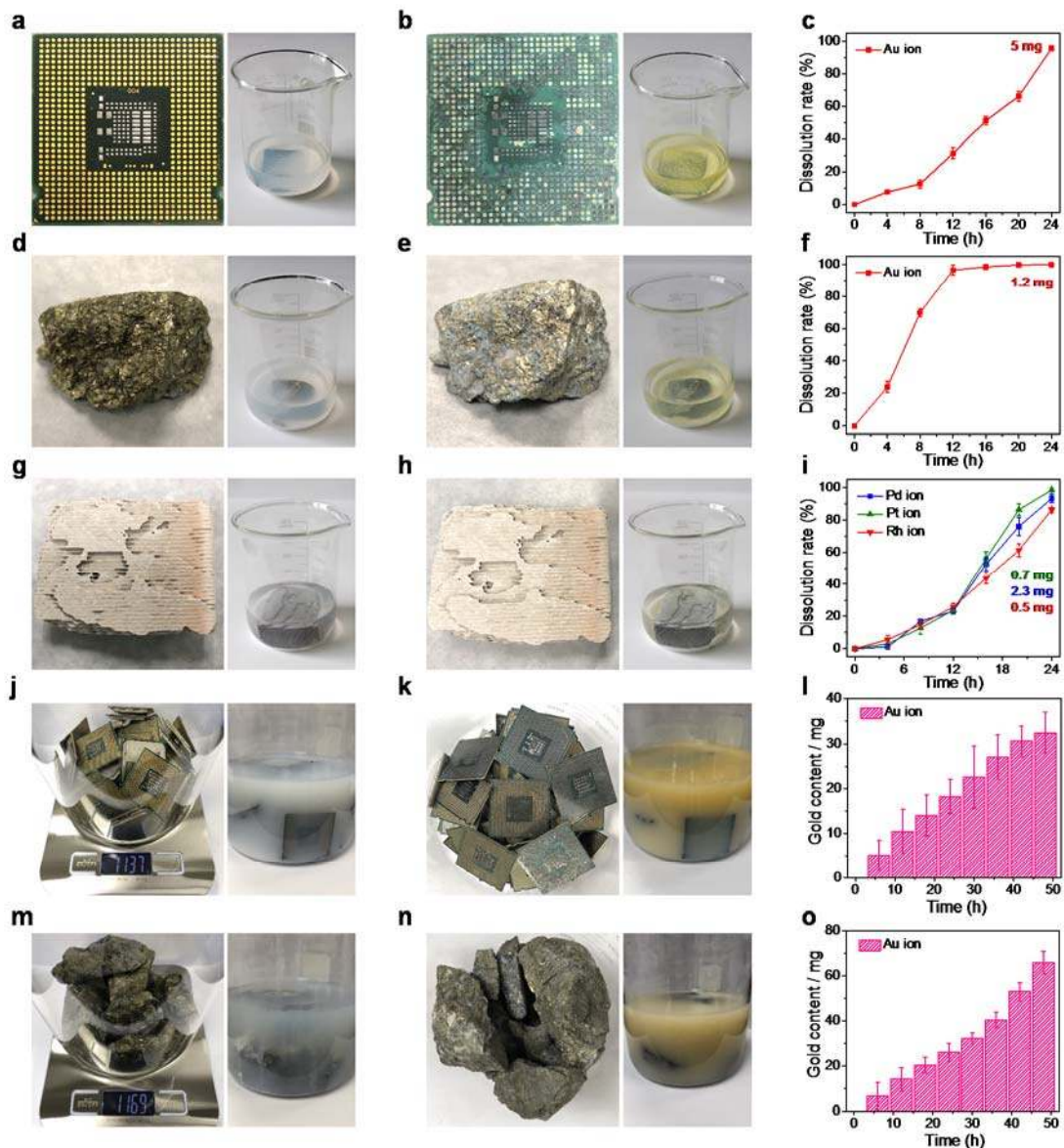86　dissolution and recovery of precious metals.

87

88　**Results**

89　**Photocatalytic Dissolution of Precious Metals**

90　　　Here, photocatalysis was used to recycle precious metals from waste electrical and

91　electronic equipment (WEEE), ore waste and three-way catalytic (TWC). As shown in

92　**Fig. 1**, gold (Au) from central processing unit (CPU) board (**Fig. 1a-1c**) and gold ore

93　(**Fig. 1d-1f**) was successfully dissolved by light irradiation, as well as palladium (Pd),

94　platinum (Pt) and rhodium (Rh) contained in TWC (**Fig. 1g–1i**). The required reaction

95　conditions are mild and the raw materials can be simply added and mixed (**Extended**

96　**Data Fig. 1**). By crushing the bulk samples, the reaction contact surface can be

97　increased and more metals will be dissolved out (**Extended Data Fig. 2**). As shown in

98　**Extended Data Fig. 3**, there are several metals such as copper (Cu), nickel (Ni) and

99　gold (Au) in the CPU board. In the process of photocatalytic dissolution, these non-

100　noble metals can also be dissolved (**Extended Data Fig. 4)**. Compared with the aqua

101　regia method, the photocatalytic process has a mild reaction. The dissolution process of

102　aqua regia reacts violently and produces a large amount of toxic and harmful substances,

103　such as chlorine. The fracture of CPU block was seriously cracked (**Extended Data**

104　**Fig. 5**).

105　**Scalability Dissolution of Precious Metals**

106　　　The whole dissolution process is very simple, and the scale of the experiment can

107　be easily increased to the kilogram level. Take CPU and gold ore as examples (**Fig. 1j–**

108　**1o**), we used 1.137 kg of CPU board and 1.169 kg of ore respectively. With the increase

109　of reaction time, the content of gold in the solution increased gradually. The color of

110　the solution showed the yellow characteristic of gold ions. These showed that the
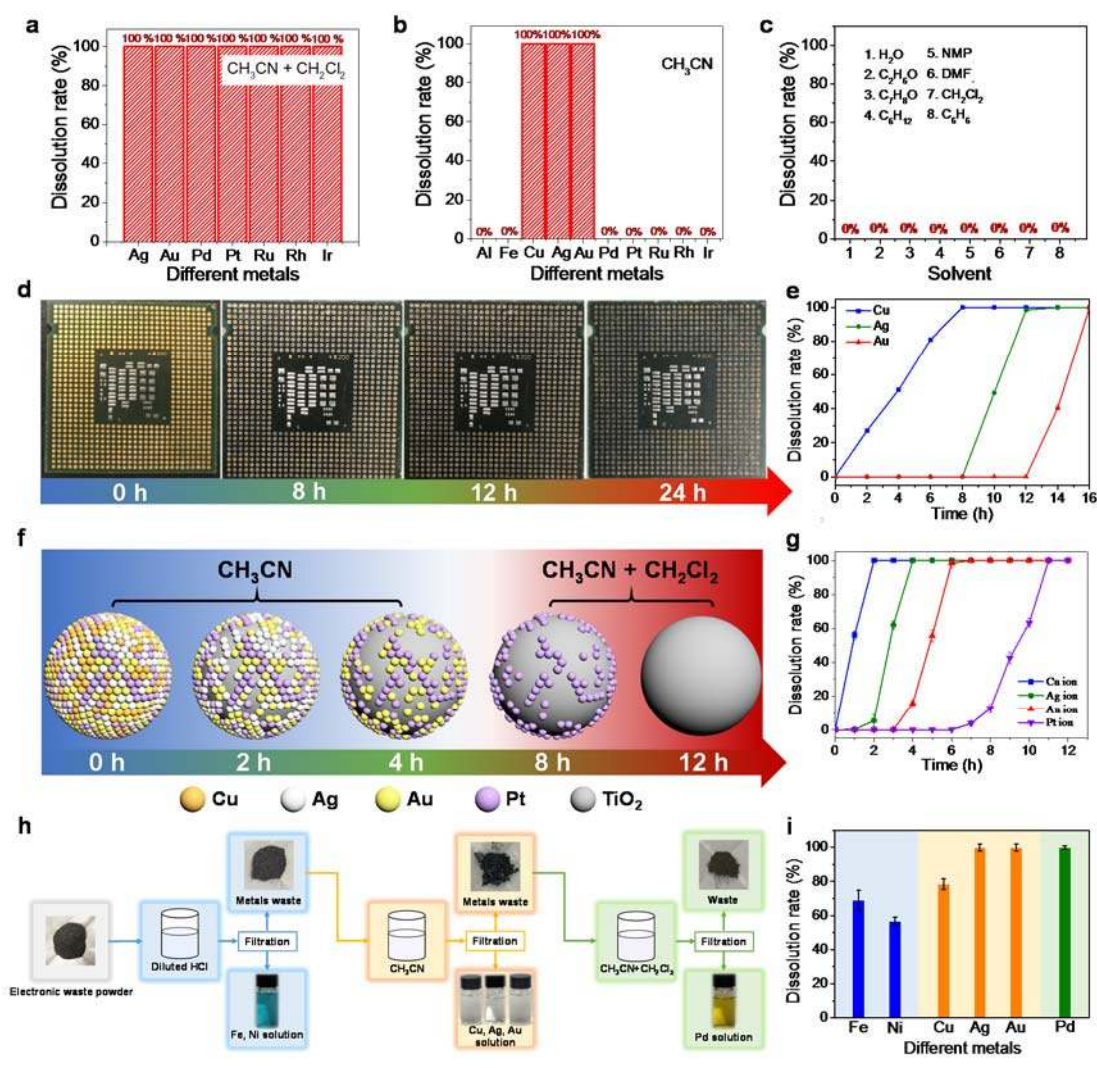
111　method is feasible in scale-up.

112

**Figure 1 | Photocatalytic dissolution of precious metals from CPU board, gold ore and TWC.** Photographs of retrieving gold from CPU board (a) before and (b) after reaction. Photographs of retrieving gold from gold ore (28.8 g) (d) before and (e) after reaction. Photographs of retrieving precious metals from TWC (17.9 g) (g) before and (h) after reaction. Photographs of retrieving gold from CPU board (1.137 kg) (j) before and (k) after reaction. Photographs of retrieving gold from ore (1.169 kg) (m) before and (n) after reaction. The amount of precious metals obtained by photocatalyzing unbroken CPU board (c) (l), gold ore (f) (o) and TWC (i).

121

**Selective Dissolution of Precious Metals**

122

123     We investigated the dissolution rate of different solvents for different metals under

124  photocatalytic conditions. In the mixed system of acetonitrile (MeCN) and

125  dichloromethane (DCM), 7 kinds of precious metals (Au, Ag, Pd, Pt, Ru, Rh and Ir)

126  can be effectively dissolved under light irradiation **(Fig. 2a and Extended Data Fig.**

127  **6**). While only Au, Ag and Cu can be dissolved in MeCN under the same conditions.

128  **(Fig. 2b**). Through screening 9 kinds of common solvents, it is found that only MeCN

129  can be used as solvent to realize this dissolution process (**Fig. 2c**). The selective

130  dissolution of precious metals was achieved by adjusting the reaction solvent and

131  reaction time. Taking the CPU board as the research object, the results showed that Cu,

132  Ag and Au on CPU board dissolved step by step with the increase of irradiation time

133  (**Fig. 2d-2e**).

134     To evaluate the selectivity of photocatalytic dissolution, $TiO_2$ samples loaded with

135  commonly used metals Cu, Ag, Au and Pt were selected as the research object. As

136  shown in **Figure 2f and 2g**, we sequentially dissolved Cu, Ag and Au in MeCN by

137  controlling the reaction time, then Pt is further dissolved by adding DCM. Finally, we

138  choose the e-waste powder, which contains Fe, Ni, Cu, Ag, Au and Pd. By adjusting

139  the solvent and reaction time, we can selectively recover the precious metals Ag, Au

140  and Pd (**Fig. 2h-2i**).

**Figure 2 | Photocatalytic selective dissolution of metals.** (a) Dissolution rate of Ag, Au, Pd, Pt, Ru, Rh and Ir in the mixed system of MeCN and DCM under photocatalytic conditions. (b) Dissolution rate of Al, Fe, Cu, Ag, Au, Pd, Pt, Ru, Rh and Ir in MeCN under photocatalytic conditions. (c) Dissolution rate of Au in different solution. (d) Photographs of selective retrieving metal from CPU board. (f) Schematic diagram of selective dissolution process of metals catalyst (1% Cu/$TiO_2$, 1% Ag/$TiO_2$, 1% Au/$TiO_2$ and 1% Pt/$TiO_2$). (h) Flow-sheet of stepwise extraction of Fe, Ni, Cu, Ag, Au and Pd from e-waste powder. The amount of metals obtained by selective photocatalyzing (e) CPU board, (g) metals catalyst and (i) e-waste powder.

**Reduction Recovery of Precious Metal Ion**

153        There are many ways to reduce $PM^{x+}$ to $PM^0$, such as hydrogen reduction, thermal

154    reduction, and reducing agents. Here, we choose the simplest hydrogen reduction

155    method, which can directly obtain the precious metals. The reduction process is divided

156    into two steps: the first is to recycle the solvent, and the second is to reduce the

157    precipitated solid to the precious metal. (**Fig. 3a-3d**). The analysis shows that the purity

158    of the recovered precious metals is more than 98% (**Fig. 3e-3h**). Scanning electron

159    microscopy (SEM) shows that the precious metals are nanoparticles (**Fig. 3i-3l**). X-ray

160    diffraction (XRD) further proved that these samples were metal Ag, Au, Pt and Pd,

161    respectively (**Fig. 3m-3p**).
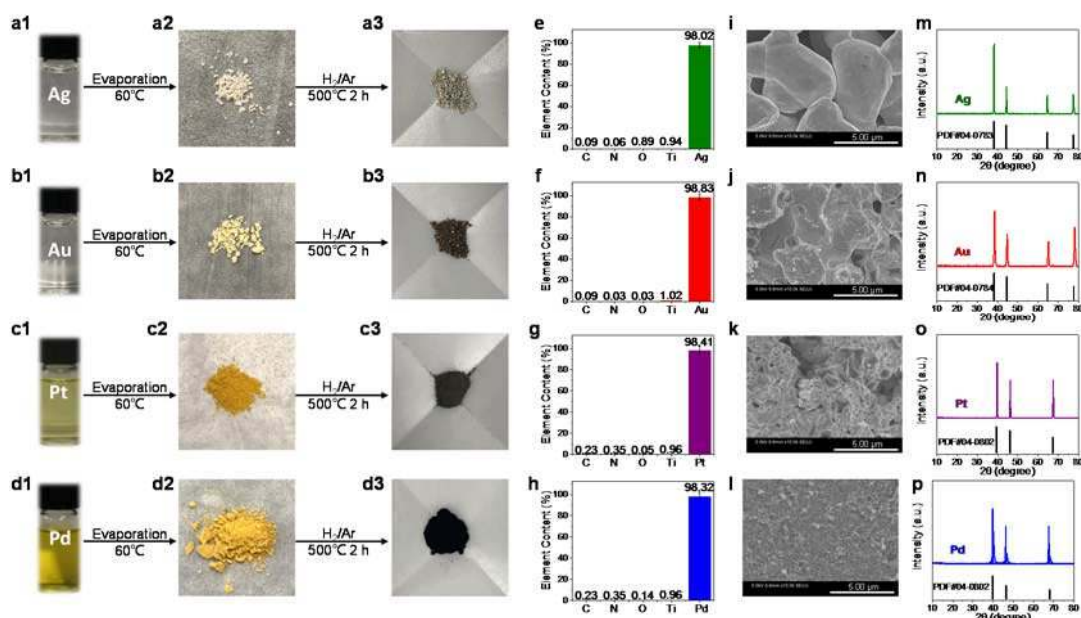


162

163    **Figure 3 | Precious metal ion reduction process.** The solvent of the dissolved product

164    is removed and then calcined in a reducing atmosphere to obtain metal (**a**) Ag, (**b**) Au,

165    (**c**) Pt and (**d**) Pd. The proportion of metal elements in the (**e**) Ag, (**f**) Au, (**g**) Pt and (**h**)

166    Pd after roasting. SEM image of the reduced product (**i**) Ag, (**j**) Au, (**k**) Pt and (**l**) Pd.

167    XRD pattern of the reduced product (**m**) Ag, (**n**) Au, (**o**) Pt and (**p**) Pd.

168

169    **Discussion**

170        In order to understand the mechanism of photocatalytic dissolution of precious

171    metals, some controlled experiments have been conducted. A commercial 5% Pt/C

172    sample is used first for photocatalyzing precious metals dissolution. Photocatalysts

173    ($TiO_2$) and precious metal catalysts (5% Pt/C) are directly mixed in solvents and stirred

174    (**Extended Data Fig. 7**). As shown in **Fig. 4a**, Pt nanoparticles are evenly distributed

175    on carbon surface. Pt nanoparticles disappeared from the surface after UV light

176    illumination (**Fig. 4b**). This can be further analyzed based on the analysis of the

177    elements in the solution, which shows that the content of Pt gradually increases in the

178    solution and Pt is completely dissolved after 4 hours (**Fig. 4g**, red line). The change of

179    Pt content on the surface was further analyzed by XPS spectra[23]. As the reaction

180    proceeded, the binding energies of $Pt^0$ $4f$ dropped substantially (**Fig. 4c**)[31]. To further

181    analyze the structure of the product, we removed the solvent from the reaction solution

182    (after reaction 4 h) and extracted the luminous the yellow powder sample (**Extended

183    Data Fig. 8a**). The infrared spectrum of the powder extracted from the solution after

184    the reaction confirmed the formation of new materials species (**Fig. 4d**). By comparing

185    the infrared spectra of the solution after the reaction, a new infrared absorption peak

186    appeared in the powder sample, located in the region of 3344–2913 cm$^{-1}$, which is a

187    typical N–H stretching vibration peak[32]. Moreover, the original C-N peak disappeared,

188    which indicates that MeCN can react to form a substance containing N-H bond during

189    the dissolution process[33]. X-ray diffraction (XRD) analysis of powder samples showed

190    that the diffraction of (($NH_4$)$_x$$PtCl_y$) sample has the hexachloroplatinate structure

191    (($NH_4$)$_2$$PtCl_6$) (PDF#07-0218)) (**Fig. 4e**). Compared with the commercial ($NH_4$)$_2$$PtCl_6$,

192    the powder samples have similar colors and XRD peak shapes (**Extended Data Fig.

193    8b-8c**). The N-H peak in powder infrared should be the amino vibration peak in this

194    sample. Energy disperse spectroscopy (EDS) mapping analysis demonstrated that there

195    were only three elements (N, Cl, Pt) in powder samples (**Extended Data Fig. 9**), which

196    is consistent with the results of XRD. X-ray photoelectronic spectroscopy (XPS)

197    analysis further showed that the valence states of platinum in the sample were mainly

198    tetravalent and divalent ($Pt^{4+}$ (73.4 eV and 75.3 eV) and $Pt^{2+}$ (76.7 eV and 78.6 eV))

199    (**Fig. 4f**)[34]. The N and Cl elements also exhibit corresponding peaks of N-H and Pt-Cl

200    (**Extended Data Fig. 10**). Through electron paramagnetic resonance (EPR) test of the

201    solution, the valence states of platinum in the sample might also have a small amount

202   of $Pt^+$ or $Pt^{3+}$ (**Extended Data Fig. 11**)[35]. From the valence state of Pt, it shows that Pt

203   has been oxidized from $Pt^0$ to $Pt^{4+}$.

204       Platinum nanoparticles (Pt NPs) on different supports ($SiO_2$, $Al_2O_3$ and molecular

205   sieve) can be dissolved by photocatalytic technology (**Extended Data Fig. 12**). The

206   main function of the $TiO_2$ is to produce active species under light irradiation. Other

207   photocatalysts, such as ZnO (under UV light irradiation) or CdS (under visible light

208   irradiation), can also realize the dissolution of Pt NPs (**Extended Data Fig. 13**).

209   Through the study of the content and change of various solvents, it indicates the

210   importance of cyano group and chloric substituent (**Extended Data Fig. 14**). The

211   aqueous solution of ammonium chloride cannot dissolve Pt NPs through photocatalytic

212   technology, and the inorganic chloride is also ineffective for the dissolution of Pt NPs

213   (**Extended Data Fig. 15**). The control experiments indicate that the presence of oxygen,

214   UV light, and photocatalyst is essential for Pt NPs dissolution (**Fig. 4g**). According to

215   the dissolution efficiency of capturing electrons (the superoxide radicals ($\bullet O_2^-$) formed

216   by the combination with oxygen) and holes (**Fig. 4h**), the photogenerated electrons and

217   holes are the main active charge carriers.

218       In addition, the $\bullet O_2^-$ and methyl radicals ($\bullet CH_2R$) generated during the reaction

219   were further verified by ESR test (**Extended Data Fig. 16a**). Under the condition of no

220   photocatalyst, free radical is not detected (**Extended Data Fig. 16b**). Further, the

221   content of hydrogen peroxide ($H_2O_2$) in the system was not detected by the iodometric

222   method, proving that the superoxide radical has not been converted to $H_2O_2$ (**Extended

223   Data Fig. 17**). Through a comprehensive analysis of the dissolution system, acetylene

224   was found in the gas phase (**Extended Data Fig. 18**). The experiments of discolored

225   silica gel were used to prove that there was water in the solution after reaction, and the

226   water content in the dissolution reaction is quantitatively detected by Karl Fischer

227   analysis. (**Extended Data Fig. 19**).

228       Based on the above results, the reaction mechanism of the photocatalyzing

229   dissolution process is proposed in **Fig. 4i**. Photogenerated electrons and holes on $TiO_2$

230   are first excited by UV light (stage 1). Photogenerated electrons react with oxygen

231     molecules to form $\cdot O_2^-$ (stage 2)[36]. Holes react with MeCN in mixed solvents to

232     deprotonate into $\cdot$CHCN radical (stage 2). DCM decomposes into $\cdot CH_2Cl$ with strong

233     oxidizing ability under the excitation of light (stage 3). These active species oxidize

234     $PM^0$ to form $PM^{x+}$ (stage 4). At the same time, the solvent is decomposed into acetylene,

235     amino group and water. Finally, the ions coordinate with each other to form

236     $(NH_4)_x PMCl_y$ (stage 5). The dissolved products of Cu and Au also have similar

237     compound structures, which further verifies the reliability of the mechanism. The XPS

238     spectra of Cu and Au show that the metal is ionized after dissolution (**Extended Data**

239     **Fig. 20a and 20b**). The XRD patterns of Cu compound correspond ammonium

240     chlorocuprate $((NH_4)_2CuCl_4 \cdot 2H_2O)$ (**Extended Data Fig. 20c**). It can be shown that the

241     Au product should be $(NH_4)_x AuCl_y$ by data fitting (**Extended Data Fig. 20d**). The

242     oxidation potential and coordination environment were changed by the regulation of

243     solvent. Therefore, the selective dissolution of Cu, Ag and Au in MeCN can be realized

244     by adjusting the solvent.



245
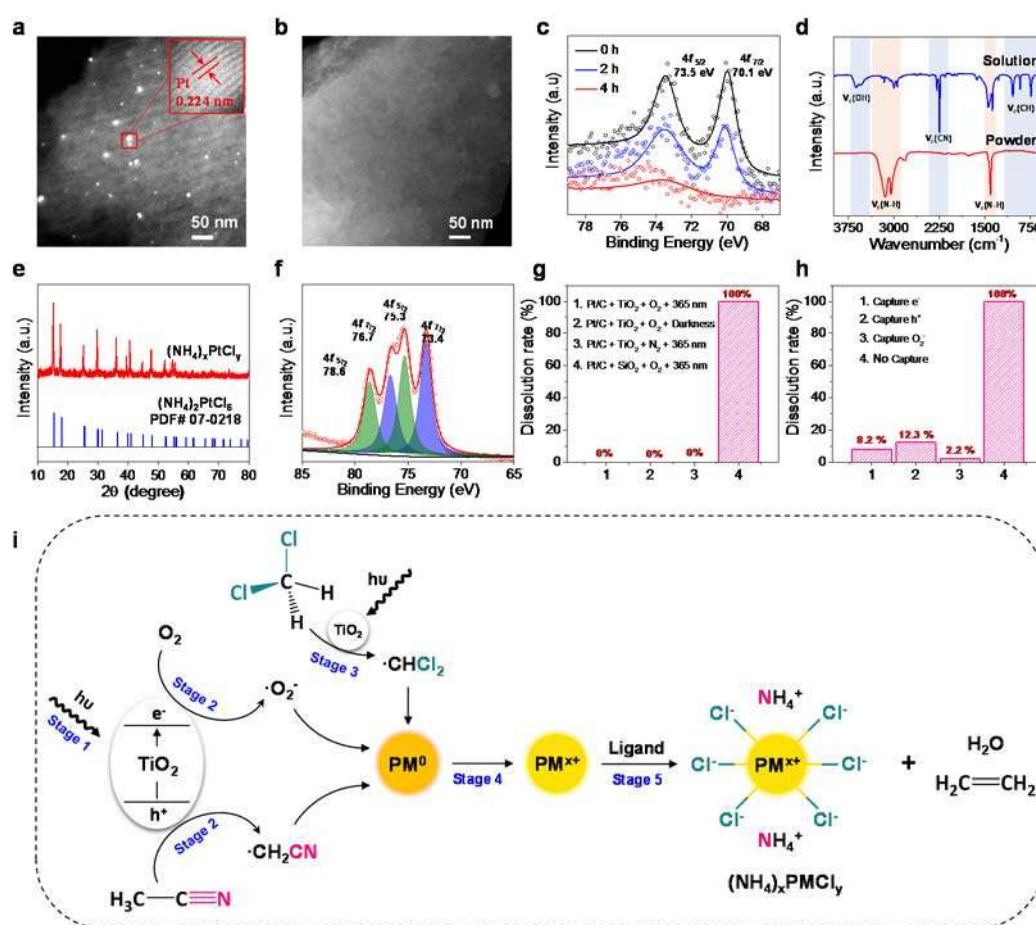
246 **Figure 4 | Exploration of mechanism.** High-angle annular dark-field (HAADF)

247 scanning transmission electron microscopy (STEM) images of 5% Pt/C (a) before and

248 (b) after reaction. (c) The Pt element distribution in Pt/C sample determined by XPS

249 spectra with reaction time. (d) FTIR spectra of solution and powder sample after

250 reaction. (e) XRD patterns and (f) Pt 4$f$7 XPS spectra of Pt compound obtained from

251 the solution. (g) Dissolution rate of Pt under different conditions. (h) Dissolution rate

252 of Pt under the capture of different living species (DDQ capture electrons (e$^-$), EDTA-

253 2Na capture holes (h$^+$), p-benzoquinone capture superoxide radical ($\cdot O_2^-$)). (i) Proposed

254 mechanism for the retrieving precious metal by photocatalysis.

255     In this work, we are able to take the advantage of the photocatalytic oxidation

256 technology to solve the complete and selective dissolution of precious metals under

257 mild conditions. We realized the oxidation leaching of precious metal ions from e-waste,

258 ore and TWC, and then recovered the precious metals. The method is simple, mild and

259 environmentally friendly, and is suitable for all kinds of precious metals. It indicated

260 that the whole reaction process is stable and can be recycled. The reaction solvent can

261 be continuously circulated for more than 45 times (**Extended Data Fig. 21**). In addition,

262 the photocatalyst can be recycled more than 100 times (**Extended Data Fig. 22a**). The

263 morphology and structure of the photocatalyst did not change before and after the

264 reaction (**Extended Data Fig. 22b and 22c**), and no free form of Ti ions was detected

265 in the solution after dissolution (**Extended Data Fig. 22d**). Such a general method has

266 a wide range of applications and can be applied not only to the recovery of precious

267 metals from powder nanocatalysts, but also the recovery of precious metals from WEEE,

268 mining of precious metals ores and TWC. It provides a breakthrough solution for the

269 smelting, dissolution and recovery of precious metals, and broadens the application

270 field of photocatalysis.

271

## Data availability

The data supporting the findings of the study are available within the paper and its Supplementary Information.

## References

1.  Fan, Z. & Zhang, H. Crystal phase-controlled synthesis, properties and applications of noble metal nanomaterials. *Chem. Soc. Rev.* **45**, 63-82 (2016).

2.  Zhao, M. *et al.* Metal-organic frameworks as selectivity regulators for hydrogenation reactions. *Nature* **539**, 76-80 (2016).

3.  Sean T. Hunt *et al.* Self-assemblyofnoble metal monolayers ontransition metal carbide nanoparticle catalysts. *Science* **352**, 947-978 (2019).

4.  USGS, Commodity Statistics and Information, 2017. https://minerals.usgs.gov/minerals/pubs/commodity/.

5.  Li, B. *et al.* Recovery of platinum group metals from spent catalysts: A review. *Int. J. Miner. Process.* **145**, 108-113 (2015).

6.  NIMS (National Institude for Material Science, Japan), 2015. Available at: www.nims.go.jp/jpn/news/press/pdf/press215_2.pdf.

7.  Cafer T. Yavuz *et al.* Gold Recovery from E‑Waste by Porous Porphyrin−Phenazine Network Polymers. *Chem. Mater.* **32**, 5343-5349 (2020).

8.  Liu, C. *et al.* Economic and environmental feasibility of hydrometallurgical process for recycling waste mobile phones. *Waste Manage.* **111**, 41-50 (2020).

9.  Prudence Dato. Economic analysis of e-waste market. *Int Environ Agreements.* **17**, 815-837 (2017).

10. Doidge, E. D. *et al.* A simple primary amide for the selective recovery of gold from secondary resources. *Angew. Chem. Int. Ed.* **55**, 12436-12439 (2016).

11. Sun, D. T., Gasilova, N., Yang, S., Oveisi, E. & Queen, W. L. Rapid, selective extraction of rrace amounts of gold from complex water mixtures with a metal-organic framework (MOF)/polymer composite. *J. Am. Chem. Soc.* **140**, 16697-16703 (2018).

300    12.    Liu, Z. *et al.* Selective isolation of gold facilitated by second-sphere
301           coordination with alpha-cyclodextrin. *Nat. Commun.* **4**, 1855 (2013).

302    13.    Yue, C. *et al.* Environmentally benign, rapid, and selective extraction of gold
303           from ores and waste electronic materials. *Angew. Chem. Int. Ed.* **56**, 9331-9335
304           (2017).

305    14.    Cherevko, S. *et al.* Dissolution of noble metals during oxygen evolution in
306           acidic media. *ChemCatChem* **6**, 2219-2223 (2014).

307    15.    McGivney, E. *et al.* Biogenic cyanide production promotes dissolution of gold
308           nanoparticles in soil. *Environ. Sci. Technol.* **53**, 1287-1295 (2019).

309    16.    Birich, A., Stopic, S. & Friedrich, B. Kinetic investigation and dissolution
310           behavior of cyanide alternative gold leaching reagents. *Sci Rep* **9**, 7191 (2019).

311    17.    Ahtiainen, R. & Lundström, M. Cyanide-free gold leaching in exceptionally
312           mild chloride solutions. *J. Clean Prod.* **234**, 9-17 (2019).

313    18.    James Hutton: father of modern geology, *Nature* **119**, 1726–1797 (1927).

314    19.    Lee, H., Molstad, E. & Mishra, B. Recovery of gold and silver from secondary
315           sources of electronic waste processing by thiourea leaching. *JOM* **70**, 1616-
316           1621 (2018).

317    20.    Burdinski, D. & Blees, M. H. Thiosulfate- and thiosulfonate-based etchants for
318           the patterning of gold using microcontact printing. *Chem. Mater.* **19**, 3933-3944
319           (2007).

320    21.    Cho, E. C., Xie, J., Wurm, P. A. & Xia, Y. Understanding the role of surface
321           charges in cellular adsorption versus internalization by selectively removing
322           gold nanoparticles on the cell surface with a I$_2$/KI etchant. *Nano Lett.* **9**, 1080-
323           1084 (2009).

324    22.    Parga, J. R., Valenzuela, J. L. & T., F. C. Pressure cyanide leaching for precious
325           metals recovery. *JOM* **59**, 43–47 (2007).

326    23.    Lopes, P. P. *et al.* Dynamics of electrochemical Pt dissolution at atomic and
327           molecular levels. *J. Electroanal. Chem.* **819**, 123-129 (2018).

328   24.   Peng, Y. *et al.* Environmentally Benign, Rapid, and SelectiveExtraction of Gold
329         from Ores and Waste ElectronicMaterials. *Angew.Chem. Int. Ed.* **56**, 9331 –
330         9335 (2017).

331   25.   Hong, J. *et al.* "Organic Aqua Regia"—Powerful Liquids for Dissolving Noble
332         Metals. *Angew. Chem. Int. Ed.* **49**, 7929 –7932 (2010).

333   26.   Hong, Y. et al. Precious Metal Recovery from Electronic Waste by a Porous
334         Porphyrin Polymer. *PNAS* **117** (28), 16174-16180 (2020).

335   27.   David K. Smith. *et al.* SelectiveExtraction and In Situ Reduction ofPrecious
336         Metal Salts from Model Waste To Generate Hybrid Gels with Embedded
337         Electrocatalytic Nanoparticles. *Angew.Chem. Int. Ed.* **55**, 183 –187 (2016).

338   28.   Wendy L. Queen. *et al.* Rapid, Selective Extraction of Trace Amounts of Gold
339         from Complex Water Mixtures with a Metal−Organic Framework
340         (MOF)/Polymer Composite. *J. Am. Chem. Soc.* **140**, 48, 16697–16703 (2018).

341   29.   Wang, X. *et al.* Semiconductor Heterojunction Photocatalysts: Design,
342         Construction, and Photocatalytic Performances. *Chem. Soc. Rev.* **43**, 5234
343         (2014).

344   30.   Serhiy, C. *et al.* Dissolution of Noble Metals during Oxygen Evolution in Acidic
345         Media. *ChemCatChem* **6**(8), 2219-2223 (2014).

346   31.   Dong, C. *et al.* Size-dependent activity and selectivity of carbon dioxide
347         photocatalytic reduction over platinum nanoparticles. *Nat. Commun.* **9**, 1252
348         (2018).

349   32.   Sun, C. & Xue, D. In situ IR spectral observation of $NH_4H_2PO_4$ crystallization:
350         structural identification of nucleation and crystal growth. *J. Phys. Chem. C* **117**,
351         19146-19153 (2013).

352   33.   Ennis, C., Auchettl, R., Ruzi, M. & Robertson, E. G. Infrared characterisation
353         of acetonitrile and propionitrile aerosols under Titan's atmospheric conditions.
354         *Phys. Chem. Chem. Phys.* **19**, 2915-2925 (2017).

355   34.   Li, Y. H. *et al.* Unidirectional suppression of hydrogen oxidation on oxidized
356         platinum clusters. *Nat. Commun.* **4**, 2500 (2013).

357 35. Chaudhuri., P. *et al.* Electronic structure of bis(o-iminobenzosemiquinonato)metal complexes (Cu, Ni, Pd). The art of establishing physical oxidation states in transition-metal complexes containing radical ligands. *J. Am. Chem. Soc.* **123**, 2213-2223 (2001).

361 36. Siemer, N. *et al.* Atomic scale explanation of $O_2$ activation at the Au-$TiO_2$ interface. *J. Am. Chem. Soc.* **140**, 18082-18092 (2018).

363 37. Han, G. *et al.* Visible-light-driven valorization of biomass intermediates integrated with $H_2$ production catalyzed by ultrathin Ni/CdS uanosheets. *J. Am. Chem. Soc.* **139**, 15584-15587 (2017).

366 38. Xiao, J. *et al.* Integration of Plasmonic Effects and Schottky Junctions into Metal Organic Framework Composites: Steering Charge Flow for Enhanced Visible-Light Photocatalysis. *Angew. Chem. Int. Ed.* **57**(4), 1103-1107 (2017).

369 39. Frens, G Controlled Nucleation for the Regulation of the Particle Size in Monodisperse Gold Suspensions. *Nat. Phys. Sci.* **241**, 20-22 (1973).

371 40. P. C. Lee and D. Melsel. Adsorption and Surface-Enhanced Raman of Dyes on Silver and Gold Sols. *J. Phys. Chem.* **86**, 3391-3395 (1982).

373 41. Liu, L., Gao, F., Zhao, H. & Li, Y. Tailoring Cu valence and oxygen vacancy in Cu/$TiO_2$ catalysts for enhanced $CO_2$ photoreduction efficiency. *Appl. Catal. B-Environ.* **134-135**, 349-358 (2013).

383  **Author Contributions** Y.C., M.J.X., Z.F.B. and H.X.L. conceived the idea for the
384  paper. Y.C., Z.F.B. and H.X.L. designed the experiments. Y.C., J.Y.W., Y.W.
385  synthesized the material. Q.F.Z., Y.D., X.C. and Z.L.W. performed the HAADF STEM
386  images. Y.C. performed the sample characterization. Z.F.B., Z.L.W and H.X.L.
387  conducted the experiments. Y.C., Z.F.B. and H.X.L. analyzed the data and wrote the
388  manuscript. All authors contributed to writing the paper.
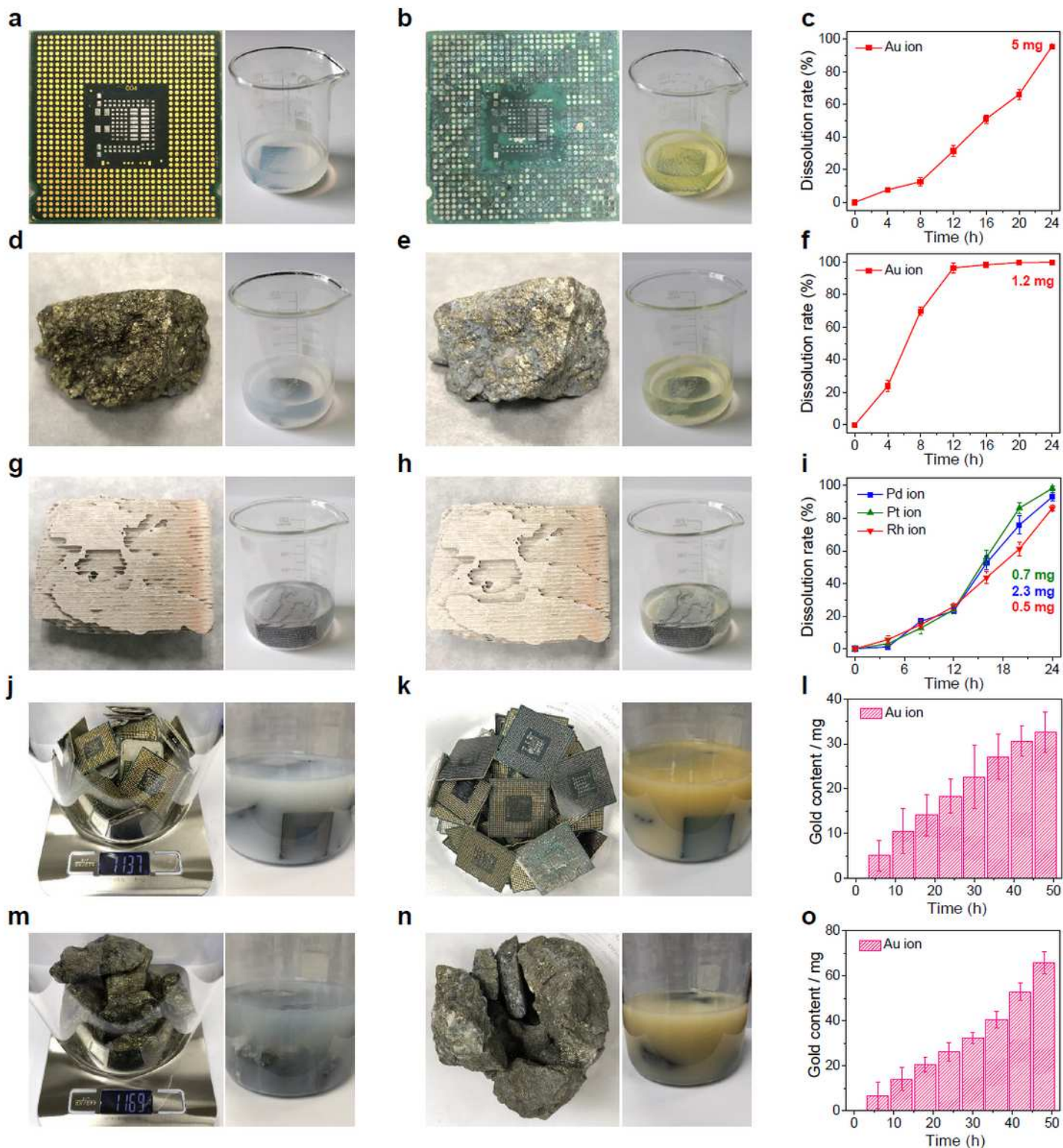
# Figures



**Figure 1**

Photocatalytic dissolution of precious metals from CPU board, gold ore and TWC. Photographs of retrieving gold from CPU board (a) before and (b) after reaction. Photographs of retrieving gold from gold ore (28.8 g) (d) before and (e) after reaction. Photographs of retrieving precious metals from TWC (17.9

g) (g) before and (h) after reaction. Photographs of retrieving gold from CPU board (1.137 kg) (j) before and (k) after reaction. Photographs of retrieving gold from ore (1.169 kg) (m) before and (n) after reaction. The amount of precious metals obtained by photocatalyzing unbroken CPU board (c) (l), gold ore (f) (o) and TWC (i).
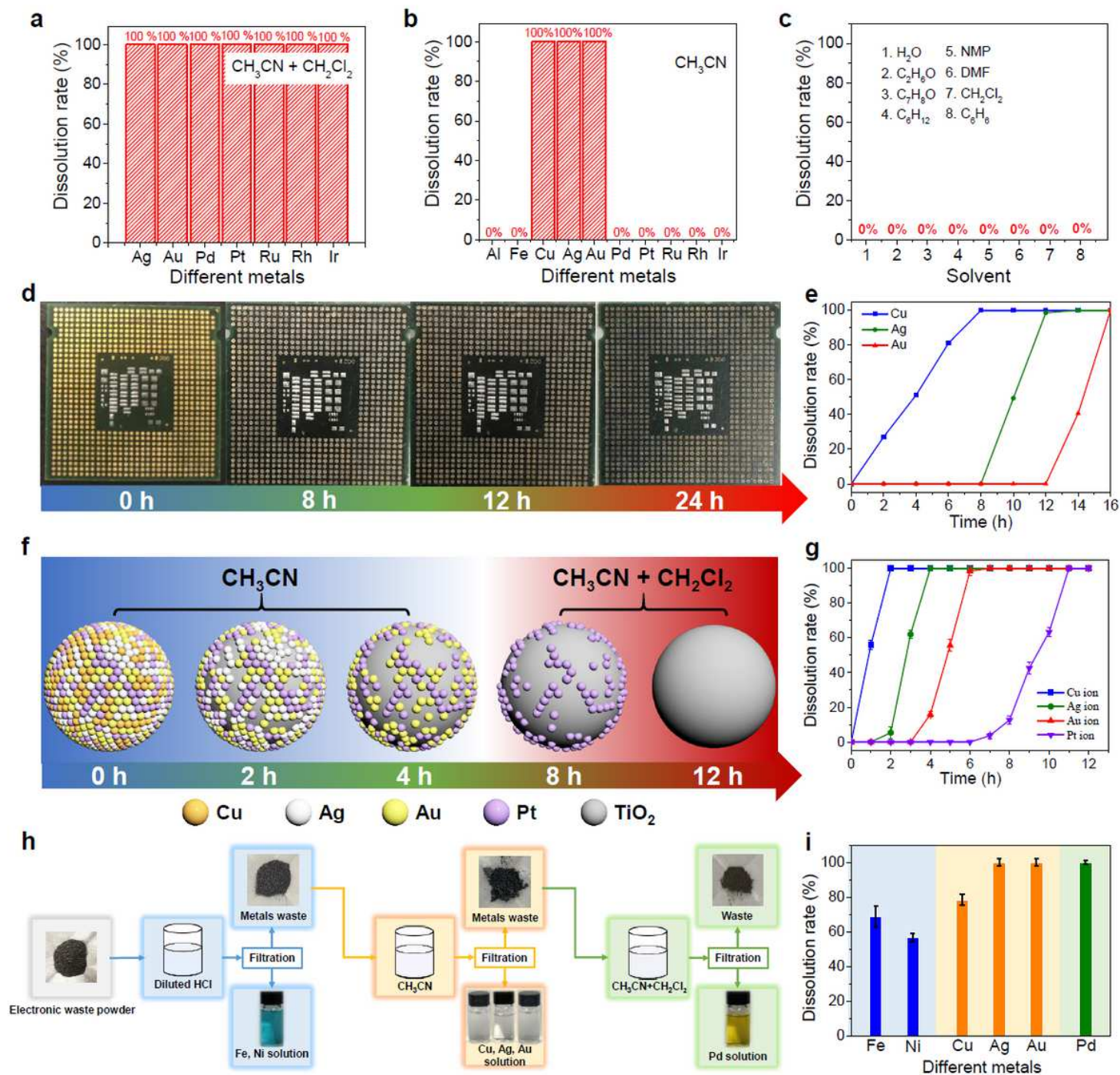


**Figure 2**

Photocatalytic selective dissolution of metals. (a) Dissolution rate of Ag, Au, Pd, Pt, Ru, Rh and Ir in the mixed system of MeCN and DCM under photocatalytic conditions. (b) Dissolution rate of Al, Fe, Cu, Ag, Au, Pd, Pt, Ru, Rh and Ir in MeCN under photocatalytic conditions. (c) Dissolution rate of Au in different

solution. (d) Photographs of selective retrieving metal from CPU board. (f) Schematic diagram of selective dissolution process of metals catalyst (1% Cu/TiO2, 1% Ag/TiO2, 1% Au/TiO2 and 1% Pt/TiO2). (h) Flow-sheet of stepwise extraction of Fe, Ni, Cu, Ag, Au and Pd from e-waste powder. The amount of metals obtained by selective photocatalyzing (e) CPU board, (g) metals catalyst and (i) e-waste powder.
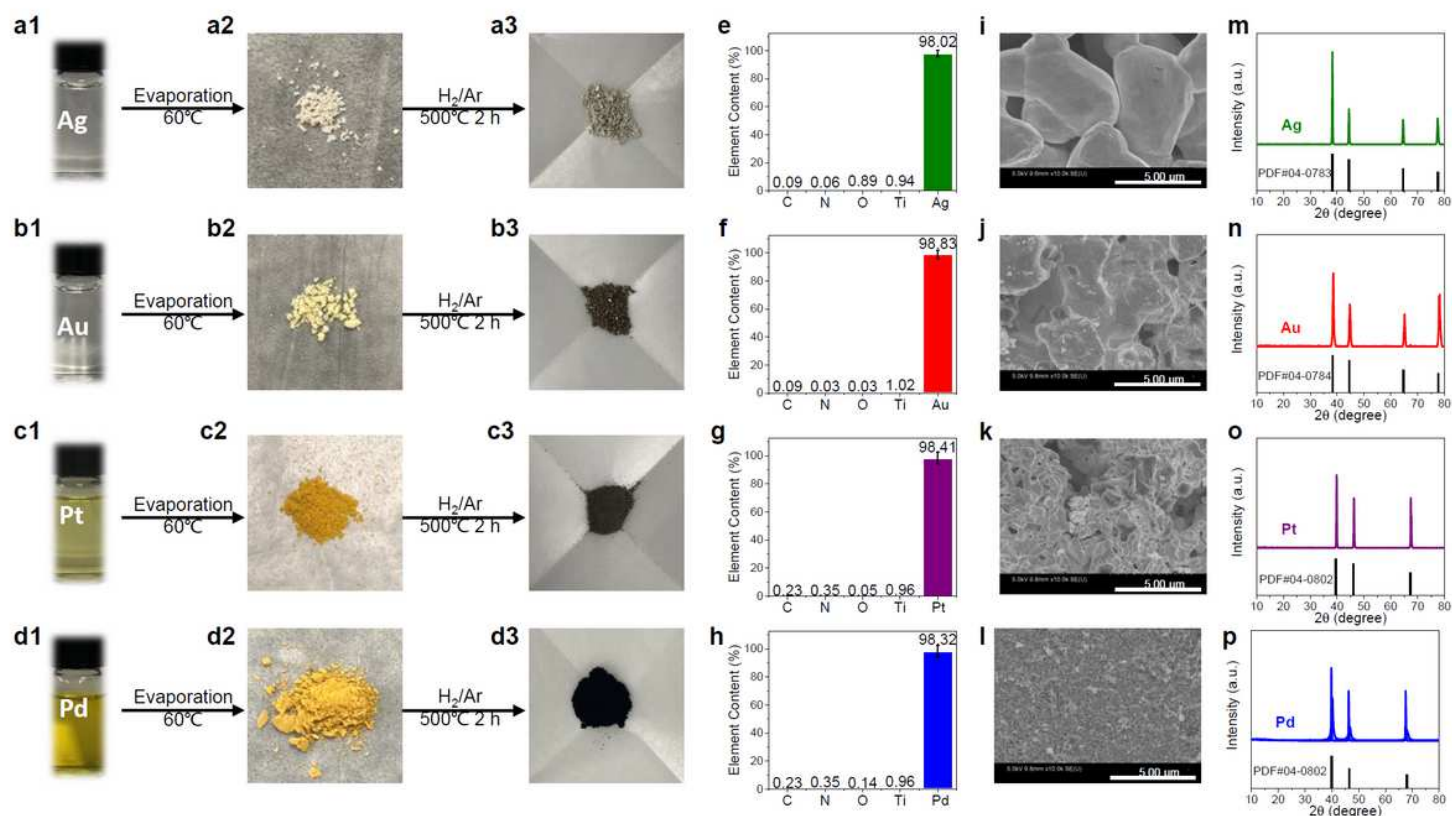


**Figure 3**

Precious metal ion reduction process. The solvent of the dissolved product is removed and then calcined in a reducing atmosphere to obtain metal (a) Ag, (b) Au, (c) Pt and (d) Pd. The proportion of metal elements in the (e) Ag, (f) Au, (g) Pt and (h) Pd after roasting. SEM image of the reduced product (i) Ag, (j) Au, (k) Pt and (l) Pd. XRD pattern of the reduced product (m) Ag, (n) Au, (o) Pt and (p) Pd.
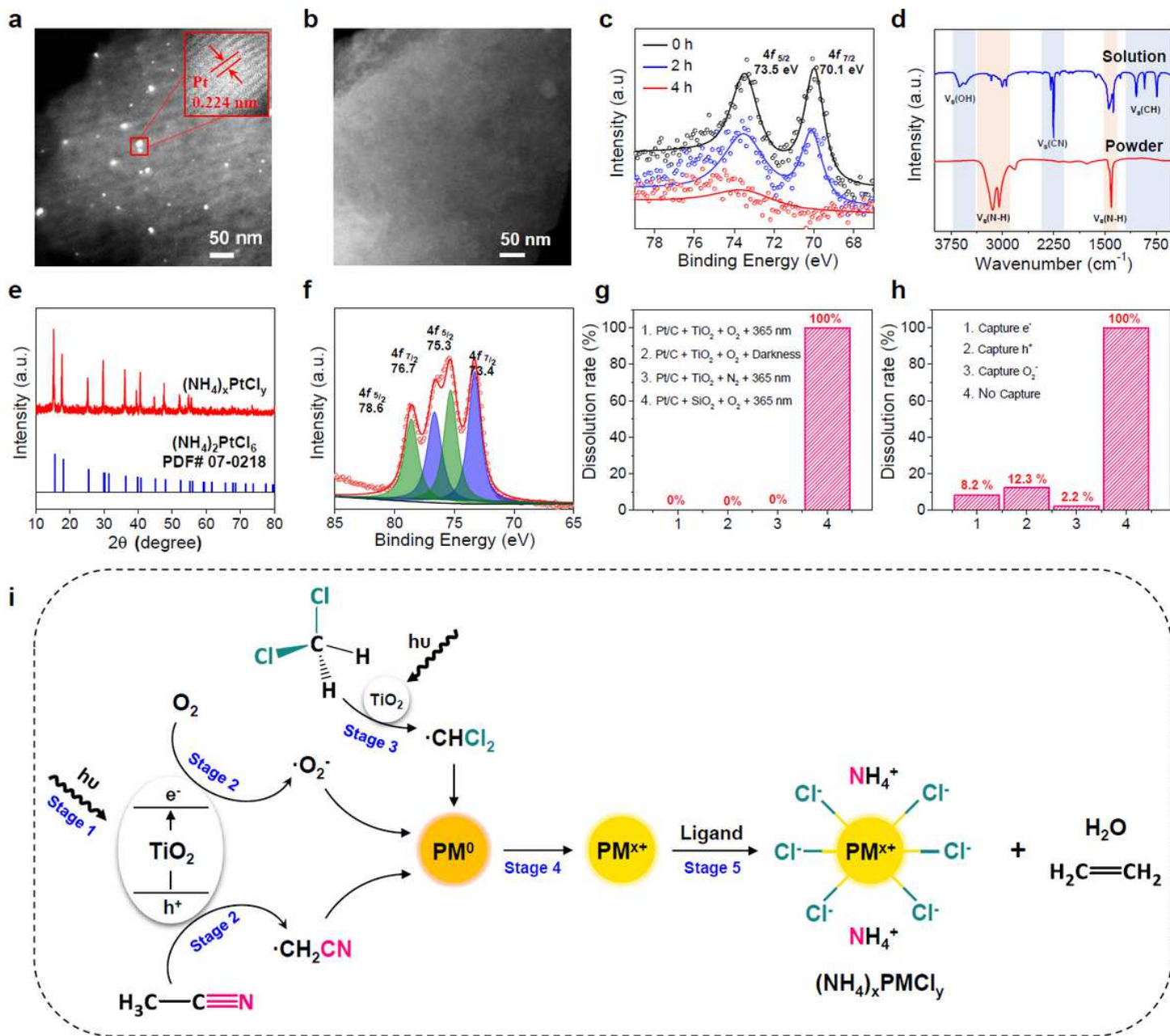
**Figure 4**

Exploration of mechanism. High-angle annular dark-field (HAADF) scanning transmission electron microscopy (STEM) images of 5% Pt/C (a) before and (b) after reaction. (c) The Pt element distribution in Pt/C sample determined by XPS spectra with reaction time. (d) FTIR spectra of solution and powder sample after reaction. (e) XRD patterns and (f) Pt 4f7 XPS spectra of Pt compound obtained from the solution. (g) Dissolution rate of Pt under different conditions. (h) Dissolution rate of Pt under the capture of different living species (DDQ capture electrons (e-), EDTA- 2Na capture holes (h+), p-benzoquinone capture superoxide radical (•O2-)). (i) Proposed mechanism for the retrieving precious metal by photocatalysis.

# Supplementary Files

This is a list of supplementary files associated with this preprint. Click to download.

- Supplementaryinformation.pdf